WILLIAM C NICKUM
STATE OF WASHINGTON
23065
REGISTERED
PROFESSIONAL ENGINEER

12/7/09

ALASKA CLASS FERRY

Computational Fluid Dynamics Resistance Analysis

Prepared for: Alaska Marine Highway System • Ketchikan, AK

Ref: 06137-005-050-2 Rev. - **December 7, 2009**

Elliott Bay Design Group
Architectural & Engineering Services for the Marine Industry

PREPARED BY

Elliott Bay Design Group
5305 Shilshole Ave. NW, Ste. 100
Seattle, WA 98107

REVISIONS

REV	DESCRIPTION	DATE	APPROVED
–	Initial issue	12/7/09	WCN 23065

TABLE OF CONTENTS

PURPOSE

The purpose of this report is to summarize the results of the computational fluid dynamics (CFD) analysis of the ALASKA CLASS FERRY. The subject vessel is a 350' × 74' × 24' vehicle ferry designed for service in Prince William Sound and southeast Alaska. An estimate of vessel resistance is given, along with a formal error analysis and a comparison to the results of a parametric speed and power estimate generated using NavCAD software (Reference 1).

PROCEDURE

The general CFD procedure and simulation approach is detailed in Appendix C. The Procedure sections below highlight settings specific to this analysis.

Geometry Preparation

The CFD model is based on an existing model of the vessel (Reference 2). The vessel geometry is modeled from the main deck to baseline. The rudders and propeller shafting and struts are modeled based on the general arrangement (Reference 3). A commonly used NACA 0018 foil is chosen for the rudder section. The propeller shafting is supported by a twin strut arrangement with the struts oriented at 30° from vertical to avoid resonance with the anticipated four-bladed propeller. The strut barrel is assumed to be radiused, and a hub diameter consistent with a controllable pitch propeller is used.

Solution Mesh Generation

See Appendix A for the coordinate system definition, domain extent, and sample views of the solution mesh. The continuous simulation domain is discretized into a finite number of cells during this stage. Simulation domain extents are taken to be 1.5L forward of the vessel, 2.5L behind the vessel, 2.0D above the baseline, and 3.0D below the baseline; where L is length on the waterline and D is total hull depth. The Calculations section shows the near wall cell height calculation. The near wall cell height calculation is performed and the mesh is sized using the fastest vessel speed, as this will result in a conservative value of near wall cell height for the lower speed cases. Table 1 shows the simulation summary.

Table 1: Simulation Summary

Simulation Summary		
Description	**Number of Cells**	**Notes**
Mesh Sensitivity Study		
Very Fine Mesh	3,797,739	All sensitivity study simulations ran at 16 ft draft and 18.3 kt speed. Model is fixed (not allowed to sink or trim)
Fine Mesh	2,109,718	
Baseline Mesh	1,670,486	
Final Mesh		
Final Mesh	2,210,937	Includes transom modification. Model is fixed. Final mesh ran at 16 ft draft and 14.0, 16.0, 18.0, and 18.3 knots

Solution Convergence and Post Processing

The time history used to determine overall hull resistance convergence for the fixed, final mesh case at 18.3 knots is shown in Appendix B.

Error Analysis

See the Calculations section for the discretization error estimation.

Final Model

Once the required level of discretization is known from the error analysis, an appropriate mesh size for the final simulation can be established. Minor hullform changes related to another design aspect are made prior to the creation of the final model, and are incorporated into the final simulation. The greatest change to the hullform is a shift in the transom aft 2.0 feet while maintaining the angle of the aft run, which effectively lengthens the waterline.

Sink and Trim Model

In addition to the model fixed CFD analysis, the final mesh is allowed to sink and trim freely (2 degrees of freedom). The 2 degrees of freedom case requires the shorter 0.1 second time step to be maintained for the entire simulation for numerical stability, and also requires additional flow time for the vessel resistance to converge. These factors combine to greatly increase the computation time required, which limits the sinkage and trim case to a single vessel speed (18.3 knots).

GIVEN AND ASSUMED PARAMETERS

Model Characteristics

CFD model characteristics are summarized in Table 2. The CFD model is run at full scale to avoid any Reynolds/Froude scaling errors. Running the simulation at full scale also avoids the requirement to establish any model to ship scale correlation allowances that are typical in physical tow tank resistance testing. Figure 1 shows an isometric bottom view of the model used in all simulations, showing included appendages.

The simulation is run at a vessel speed of 14.0, 16.0, 18.0 and 18.3 knots. The 18.3 knot case is included as the estimated speed at 80% MCR in Sea State 0 using 5,000 hp main engines from the NavCAD analysis (Reference 1).

Figure 1: Isometric View of Simulation Model

Table 2: Model Particulars

Model Particulars			
Scale:	1		
LWL:	324.7 ft		
Draft(s) Analyzed:	16.0 ft		
Displacement:	146,700 ft^3		
Displacement:	4,193 LT		
Wetted Surface:	21,295 ft^2		
Appendages Included:	Skeg, Propeller Shafts and Struts, Rudders		
Velocity:		Reynolds Number:	Froude Number:
14.0 knots	23.63 ft/sec	6.08E+08	0.231
16.0 knots	27.01 ft/sec	6.95E+08	0.264
18.0 knots	30.38 ft/sec	7.82E+08	0.297
18.3 knots	30.89 ft/sec	7.95E+08	0.302

Solver Settings

For the first 15 seconds of physical flow time, a time step length of 0.1 seconds is used, which gives a local Courant number of approximately 1.5 for the average cell at the still waterline (see Calculations section).

At 15 seconds physical flow time, the time step length is changed to 0.4 seconds and the solver is switched to a second order upwind calculation and the simulation continues to run for an additional 285 seconds. Five inner iterations are used per time step. The simulations are run for a total physical flow time of 300 seconds, which at 18.3 knots corresponds to a distance of 9,267 ft (approximately 28.5 ship lengths). This allows sufficient time for the free surface to develop around the vessel, and allows the vessel drag force to converge to a steady value. Solution settings for the fixed cases are summarized in Table 3 below.

Table 3: Solution Settings

Solution Settings		
0-15 s	Time Step:	0.1 s
	Iterations per Time Step:	5
	Iterations 0-15 s	750
	Temporal Discretization:	1st Order
15-300 s	Time Step:	0.4 s
	Iterations per Time Step:	5
	Iterations 15-300 s	3,563
	Temporal Discretization:	2nd Order
Total Physical Flow Time:		300 s
Total Iterations:		4,313

RESULTS

Error Analysis

The mesh sensitivity study results indicate that the level of spatial discretization is adequate to ensure a mesh independent resistance value. The percentage change in the predicted resistance between the three mesh refinement levels is very small relative to the percentage change in the number of cells. Comparing the baseline mesh case and the very fine mesh case shows a 0.74% change in the resistance value for a corresponding 127% increase in the number of cells. Table 4 summarizes the mesh sensitivity study parameter changes.

Table 4: Mesh Sensitivity Parameters

Mesh			Force Difference	Percent Difference
Very Fine Mesh				
	Total Resistance:	**66,886** lbf	490 lbf	0.74%
	Number of Cells:	3,797,739		127%
Fine Mesh				
	Total Resistance:	**66,636** lbf	239 lbf	0.36%
	Number of Cells:	2,109,718		26%
Baseline Mesh				
	Total Resistance:	**66,396** lbf	0 lbf	0.00%
	Number of Cells:	1,670,486		0%

The calculated Grid Convergence Index (GCI) for the very fine and baseline meshes is shown in Table 5. Appendix C details the calculation of the GCI. The number of cells used in the final mesh is chosen to be close to the number of cells in the fine mesh case for the sensitivity study. The discretization error for the final model will be within the range of 0.97% to 2.67%, and is interpolated based on number of cells. Note that the total error for the final model may be larger, as iterative and modeling errors are not included in the values below. The calculated error is acceptable for this analysis.

Table 5: Discretization Error Results

Description	Number of Cells	Discretization Error (GCI)
Mesh Sensitivity Study		
Very Fine Mesh	3,797,739	**0.97%**
Baseline Mesh	1,670,486	**2.67%**
Final Mesh		
Final Mesh (estimated)	2,210,937	**2.24%**

Final Model Resistance

The vessel resistance results of the final run are compared to the still water resistance results of the speed and power prediction (Reference 1). The Taylor head wind resistance value that estimates superstructure wind resistance as calculated in the speed and power prediction is added to the CFD resistance results as the superstructure is not modeled in the CFD simulations. The drag from bilge keels, fin stabilizers, and bow thruster is not included in the NavCAD results to provide a direct comparison to the CFD results.

The CFD results show good agreement with the parametrically-derived results of the speed and power prediction. The CFD analysis predicts less vessel resistance at 18.3 knots, which is likely due to the conservative nature of the parametric resistance estimate, as well as the relatively low wave making resistance of the ALASKA CLASS FERRY in relation to the vessel database used to produce the parametric resistance estimate (this effect would increase with increasing speed). In addition, items such as appendage drag are only roughly accounted for in the parametric estimate, and tend towards over prediction of drag in the NavCAD results.

The CFD model is fixed for the 14.0, 16.0, and 18.0 knot cases, which does not account for the dynamic sinkage and trim typical for displacement vessels when underway. For a more realistic vessel resistance result, an additional 18.3 knot case is allowed to sink and trim. Figure 2 includes the results of the free to sink and trim case, which falls between the NavCAD results and the fixed model CFD results.

Table 6 shows a comparison of the CFD simulations and the parametric NavCAD results for the 18.3 knot case. Appendix B shows the predicted free surface elevation along the hull, free surface elevation contours, and streaklines along the hull.

Table 6: Simulation Results and NavCAD Comparison

Simulation Results and NavCAD Comparison- 18.3 kt case				
Description	Resistance (lbf)	Difference (lbf)	Difference (%)	Effective Power (hp)
Final Mesh (fixed case)				
Final Mesh	65,224	--	--	--
Superstructure Resistance[1]	6,722	--	--	--
Total Resistance (fixed case)	**71,946**	0	0.0%	**4,041**
Final Mesh (sink & trim case)				
Final Mesh	70,071	--	--	--
Superstructure Resistance[1]	6,722	--	--	--
Total Resistance (fixed case)	**76,793**	4,847	6.7%	**4,313**
Speed and Power Prediction				
NavCAD Predicted Resistance[2]	**78,670**	6,724	9.3%	**4,418**
1- Superstructure Resistance value taken from Reference 1 Taylor Head Wind resistance value				
2- Predicted Resistance value includes superstructure, rudder, propeller shaft, and skeg factors				

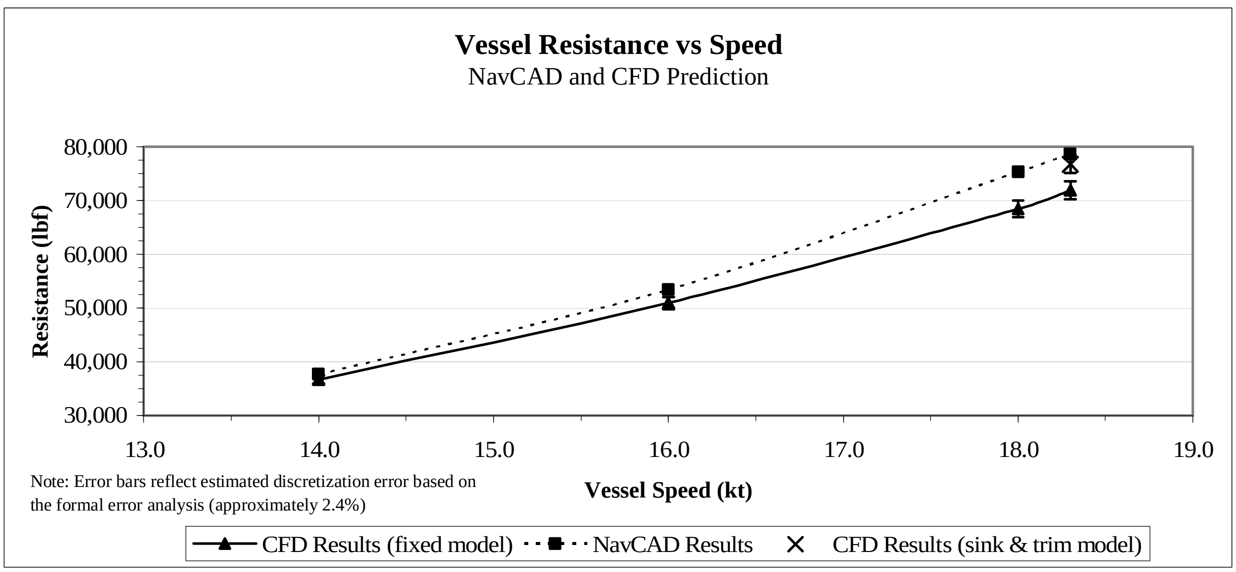

Vessel Resistance vs Speed Tabular Data						
Vessel Speed (kt)	NavCAD Results Resistance (lbf)	Base CFD Results Resistance (lbf)	Superstructure Resistance (lbf)	Corrected CFD Resistance (lbf)	Effective Power-NavCAD (hp)	Effective Power-CFD (hp)
		(fixed model)				(fixed model)
14.0	37,670	32,777	3,934	36,711	1,618	1,577
16.0	53,416	45,800	5,139	50,939	2,623	2,501
18.0	75,311	61,959	6,504	68,463	4,160	3,782
18.3	78,670	65,224	6,722	71,946	4,418	4,040
		(sink & trim model)				(sin & trim model)
18.3	78,670	70,071	6,722	76,793	4,418	4,313

Figure 2: Resistance vs. Speed Results

FUTURE WORK

As the ALASKA CLASS FERRY is still undergoing hull form changes as the design matures, it is recommended that an additional round of CFD be performed on the finalized hull form to evaluate the impacts of any geometrical changes to the vessel. Some possible items to examine are hull form modifications, active and passive roll stabilization appendages (bilge keels and/or fin stabilizers), aligned propeller shaft struts, and bow thruster.

CONCLUSIONS

The ALASKA CLASS FERRY vessel resistance at a given draft and speed range is determined using computational fluid dynamics. The results of the analysis are compared to a parametric speed and power analysis and show good agreement. The CFD results predict less resistance over the entire speed range examined, which is in line with expectations that the parametric study shows conservative results.

REFERENCES

1. Speed and Power Estimate, 06137-005-050-1, Rev. A, EBDG, October 2009.
2. ALASKA CLASS FERRY Rhino Model, 06137-005-068-1P1, EBDG, October 2009.
3. General Arrangement, 06137-005-101-1P0, EBDG, August 2009.

CALCULATIONS

Near Wall Cell Size Calculation

Values for StarCCM+

Near Wall Cell Height:	0.00391	ft	Total height of near wall cell
Resulting y+ value:	252		Must be between 30 and 300
"Number of Prism Layers":	**3**		
"Prism Layer Stretching":	**1.8**		Typical range: 1.3 to 2.0
"Prism Layer Thickness":	**0.02359**	ft	This is total prism layer height (sum of all prism layers)

Near Wall Cell Size Calculation

Required y^+ range: 30 to 300

$$y^+ = \frac{(y \times u_*)}{n}$$

y^+:	30	to	300		Dimensionless Reynolds number based on distance within the boundary layer and "friction velocity"
y:	**0.0005**	to	**0.0046**	ft	Height of the first cell off the wall

ν:	1.26E-05	ft^2/sec	Kinematic viscosity of fluid
u_*:	0.815	ft/sec	Friction velocity

$$u_* = U_e \times \sqrt{\frac{C_f}{2}}$$

U_e:	30.89	ft/sec	Free stream velocity
C_f:	**1.394E-03**		Estimated Skin friction coefficient (analogous to wall shear stress)

$$\frac{1}{\sqrt{C_f}} = 4.15 \times \log_{10}(\text{Re} \times C_f) + 1.7$$

$1/\sqrt{(C_f)}$ =	26.785	set equal by changing C_f
$4.15*\log(Re*C_f)+1.7$ =	26.785	
difference:	0.000	equals zero for correct *Cf*

Re: 7.95E+08 Reynold's Number (vessel length based)

Initial Time Step Calculation

Time Step Calculation

Δt	**0.10**	sec	to be used in Star-CCM+ as initial guess for time step, adjust as necessary
C	1.544346		target Courant Number

$$C = \frac{(U \times \Delta t)}{\Delta x}$$

U	30.89	ft/sec	free stream velocity
Δx	**2.0**	ft	average cell spacing along waterline
	162		number of cells along the waterline

Note that either cell spacing or time step may be altered to affect Courant Number. Typical approach is to mesh the hull surface to a satifactory level of discretization, then enter this spreadsheet to determine initial guess for time step.

For Implicit Unsteady calculations, the target Courant Number may be > 1, provided the solution remains numerically stable.

Minimum Physical Time

The physical time required for the vessel to travel 2x lengths
Allows vessel to physically move out of its starting wake
Note that the free surface typically requires more time to fully develop

Length	324.7	ft
Velocity	30.89	ft/sec

Minimum Solution Time: **21.0** sec

Discretization Error Calculation

The discretization error due to mesh sizing effects is calculated below following the procedure from Reference 5.

Mesh Sensitivity Cases

ΔV_{total} = 104,779,555 ft^3 total domain volume

Representative mesh size *h:* $$h = \left[\frac{1}{N}\sum_{i=1}^{N}(\Delta V_i)\right]^{1/3}$$

Very Fine

N =	3,797,739		total number of cells
h_1 =	3.02	ft	representative mesh size
Φ_1 =	66886	lbf	total resistance

Fine

N =	2,109,718		total number of cells
h_2 =	3.68	ft	representative mesh size
Φ_2 =	66636	lbf	total resistance

Baseline

N =	1,670,486		total number of cells
h_3 =	3.97	ft	representative mesh size
Φ_3 =	66396	lbf	total resistance

r = 1.31 grid refinement factor h_3 / h_1

Apparent Order of Convergence Calculation

$$p = \frac{1}{\ln(r_{21})}\left|\ln\left|e_{32}/e_{21}\right| + q(p)\right|$$ p = 6.892792

Order of convergence exceeds the theoretical limit of 2, possibly due to the localized nature of the grid refinements. To be conservative, a value of p = 2 will be used for error calculation.

$$r_{21} = h_2 / h_1$$ r_{21} = 1.2165

$$r_{32} = h_3 / h_2$$ r_{32} = 1.0809

$$q(p) = \ln\left(\frac{r_{21}^p - s}{r_{32}^p - s}\right)$$ $q(p)$ = 1.394183

$$s = 1 \cdot \mathrm{sgn}(e_{32}/e_{21})$$ s = 1

$$e_{32} = f_3 - f_2$$ ε_{32} = -239.5 lbf

$$e_{21} = f_2 - f_1$$ ε_{21} = -250.1 lbf

Extrapolated Resistance Value

This value is the resistance estimate found by extrapolating the data points to the asymptotic value. This is the theoretical resistance that would be calculated as the mesh density approaches infinity.

$$f_{ext}^{21} = (r_{21}^{p} \cdot f_1 - f_2)/(r_{21}^{p} - 1)$$ $\Phi^{21}{}_{ext} =$ 67407 lbf

Approximate Relative Error

$$e_a^{21} = \left| \frac{f_1 - f_2}{f_1} \right|$$ $e^{21}{}_{a} =$ 0.37%

Extrapolated Relative Error

$$e_{ext}^{21} = \left| \frac{f_{ext}^{21} - f_1}{f_{ext}^{21}} \right|$$ $e^{21}{}_{ext} =$ 0.77%

Fine Grid Convergence Index

This is the value used when reporting discretization error for the finest mesh.

$$GCI_{fine}^{21} = \frac{1.25 \cdot e_a^{21}}{r_{21}^{p} - 1}$$ $GCI^{21}{}_{fine} =$ **0.97%**

Coarse Grid Convergence Index

This is the value used when reporting discretization error for the coarsest mesh.

$$e_a^{32} = \left| \frac{f_2 - f_3}{f_2} \right|$$ $e^{32}{}_{a} =$ 0.36%

$$GCI_{coarse}^{32} = \frac{1.25 \cdot e_a^{32}}{r_{32}^{p} - 1}$$ $GCI^{32}{}_{coarse} =$ **2.67%**

Appendix A

Coordinate System Definition

Simulation Domain Size

Solution Mesh

Coordinate System Definition and Simulation Domain Size

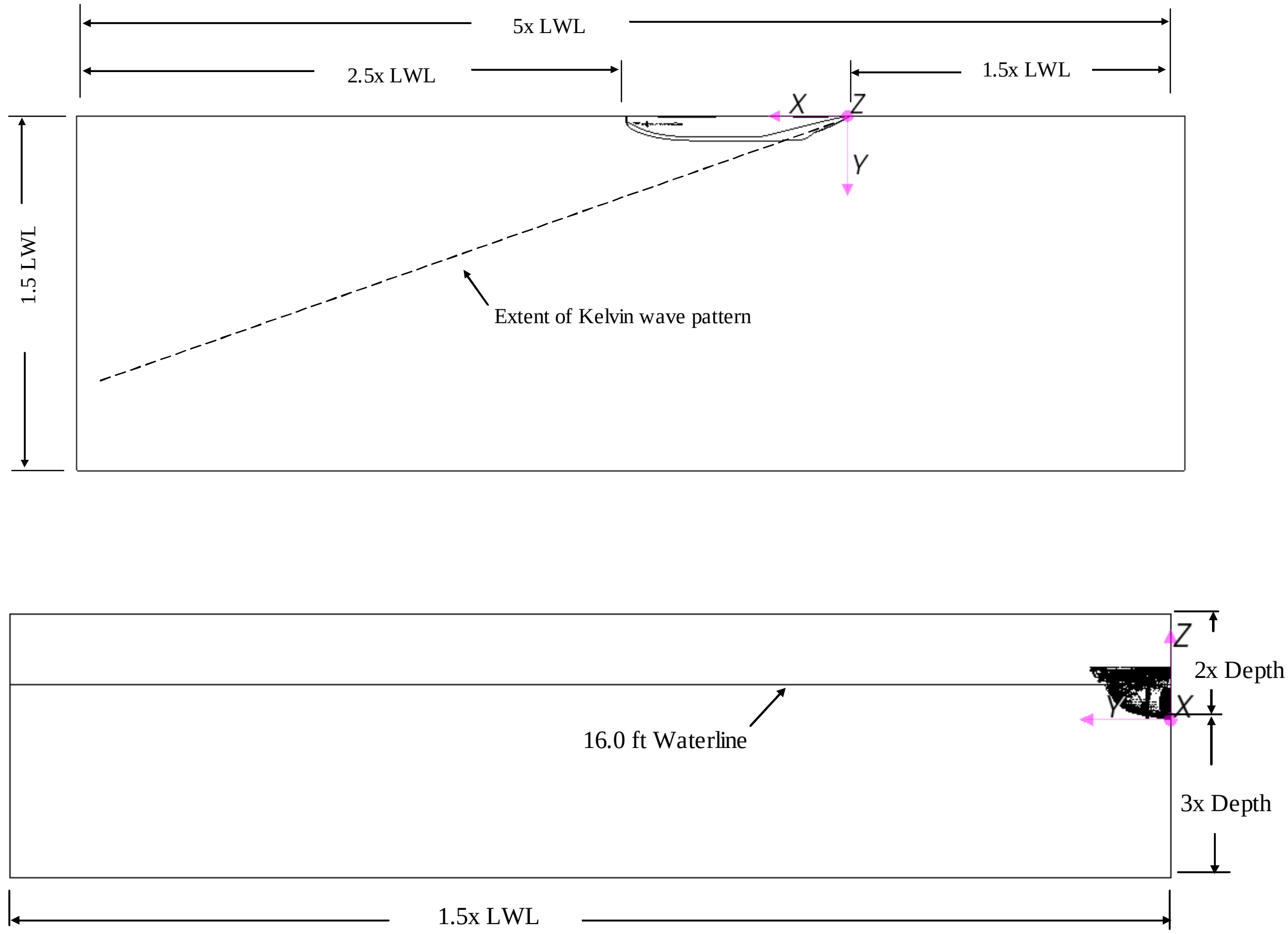

Figure A1: Simulation Domain Extents

Solution Mesh

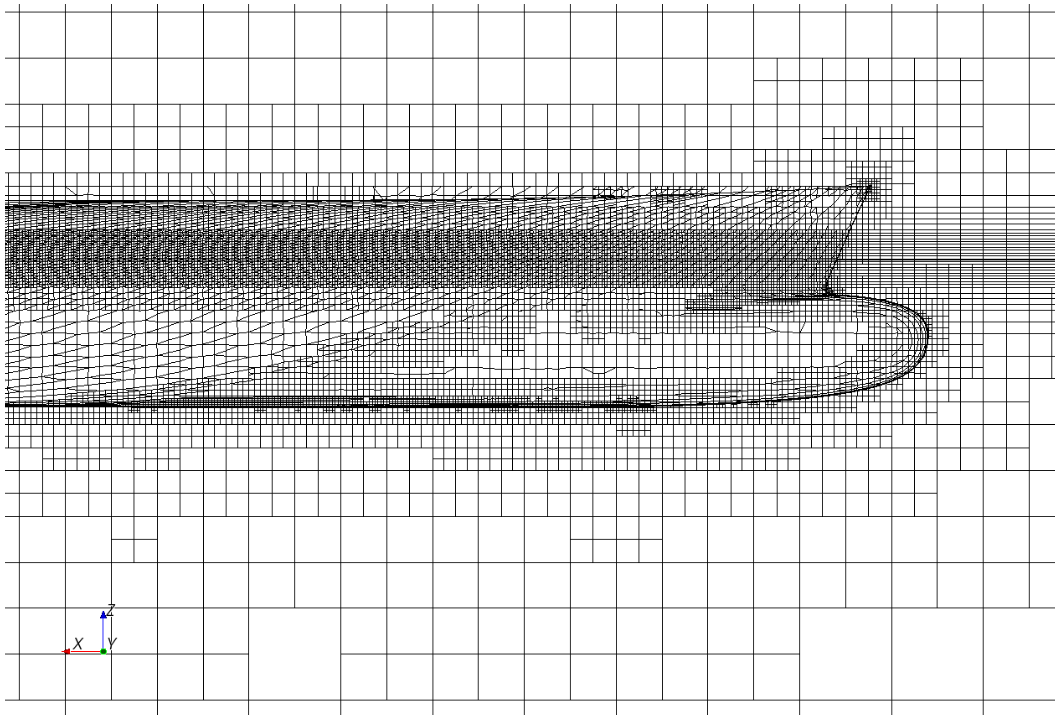

Figure A2: Solution Mesh- Bow Profile View

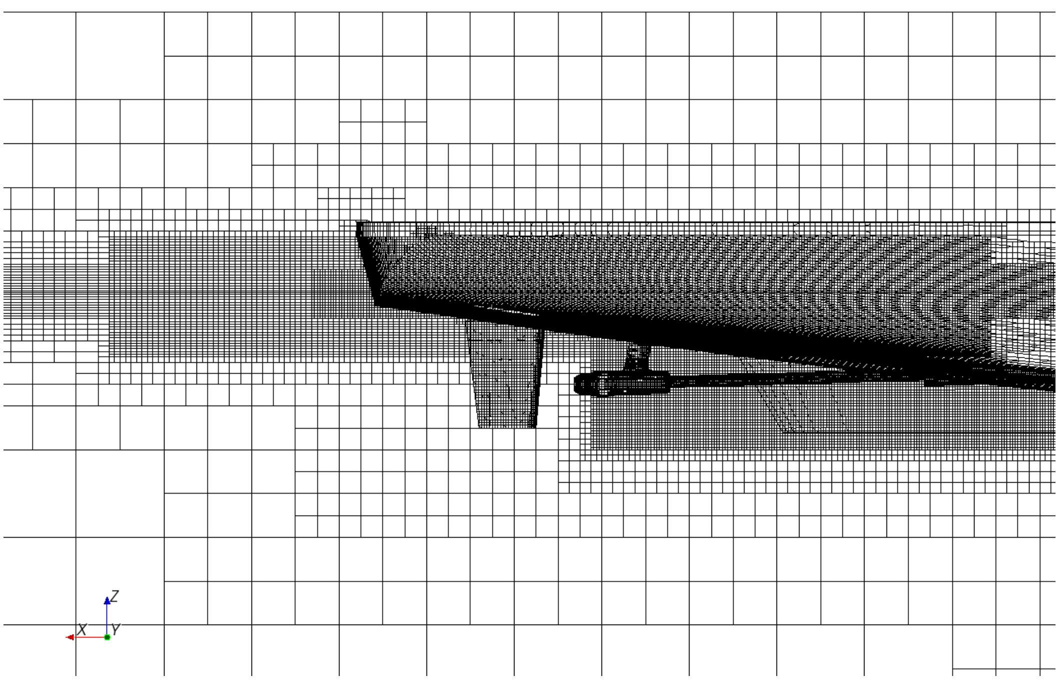

Figure A3: Solution Mesh- Stern Profile View

Note the free surface and transom refinement. The X-Z plane shown is the centerline symmetry plane. The rudder and propeller shaft have increased refinement to capture viscous wake effects (not shown).

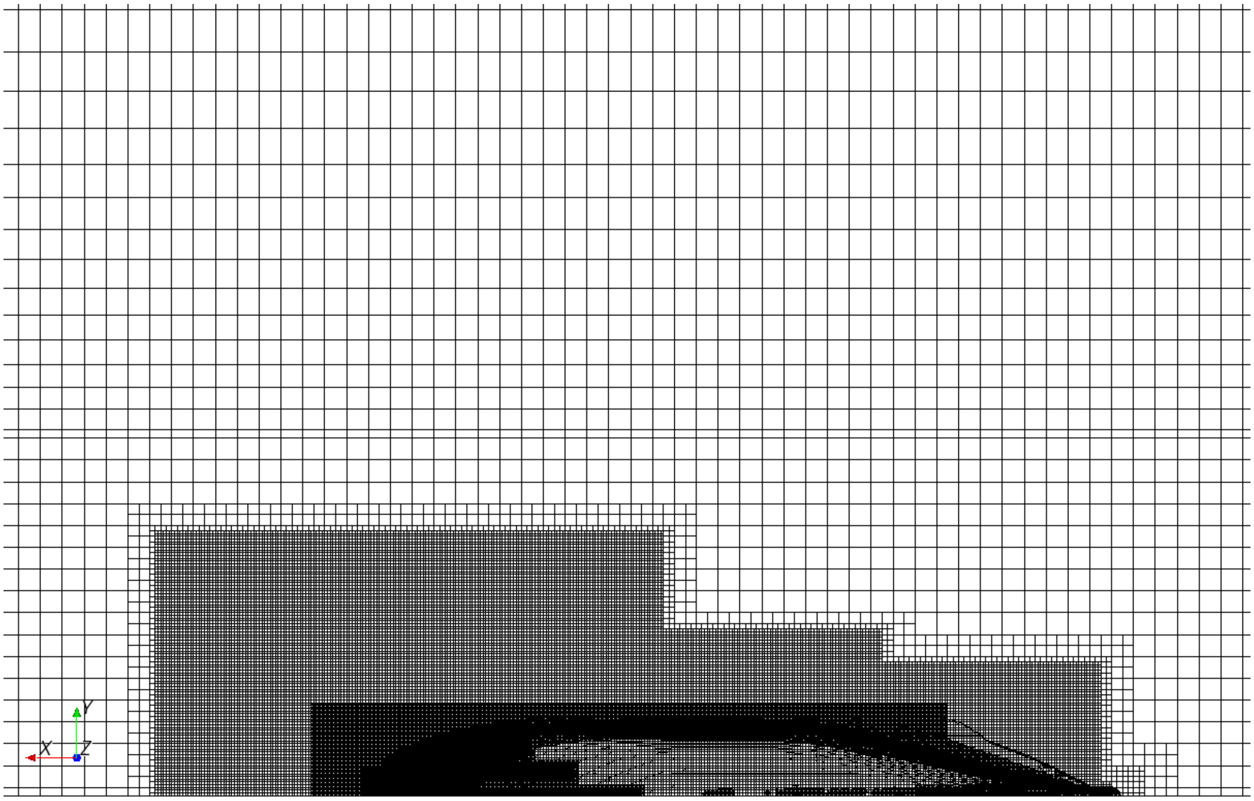

Figure A4: Solution Mesh- Plan View of Bottom of Hull

The X-Y plane shown is the still water line section through the domain. The free surface area is refined in the X-Y direction following the Kelvin wave pattern divergent angle of approximately 20 degrees from the vessel stem. The region immediately around the vessel is further refined for solution accuracy. The transverse stretching of the domain may also be seen here.

Appendix B

Resistance Convergence History

Free Surface Elevation Plot

Free Surface Elevation Contours

Hull Streaklines

Streamlines

Resistance Convergence History

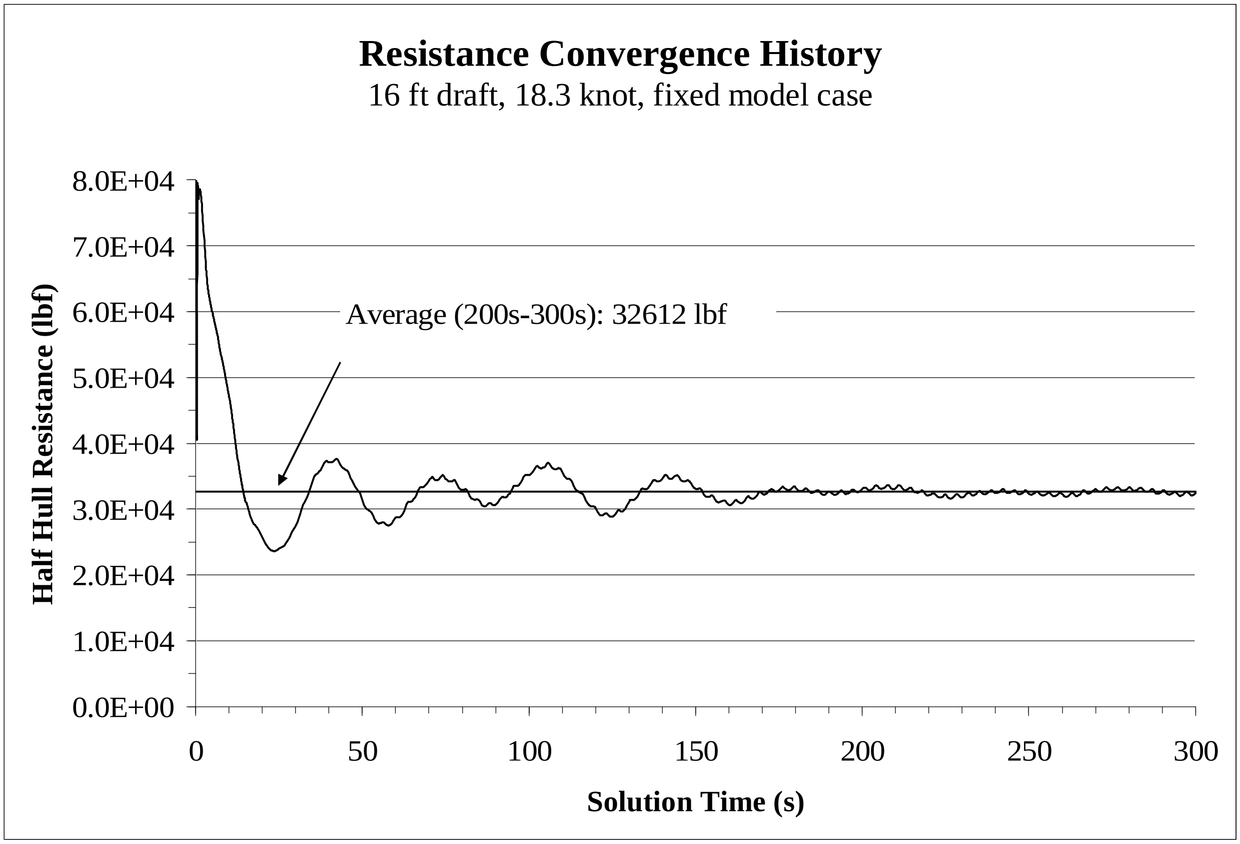

Figure B1: Sample Convergence History

Free Surface Elevation Plot

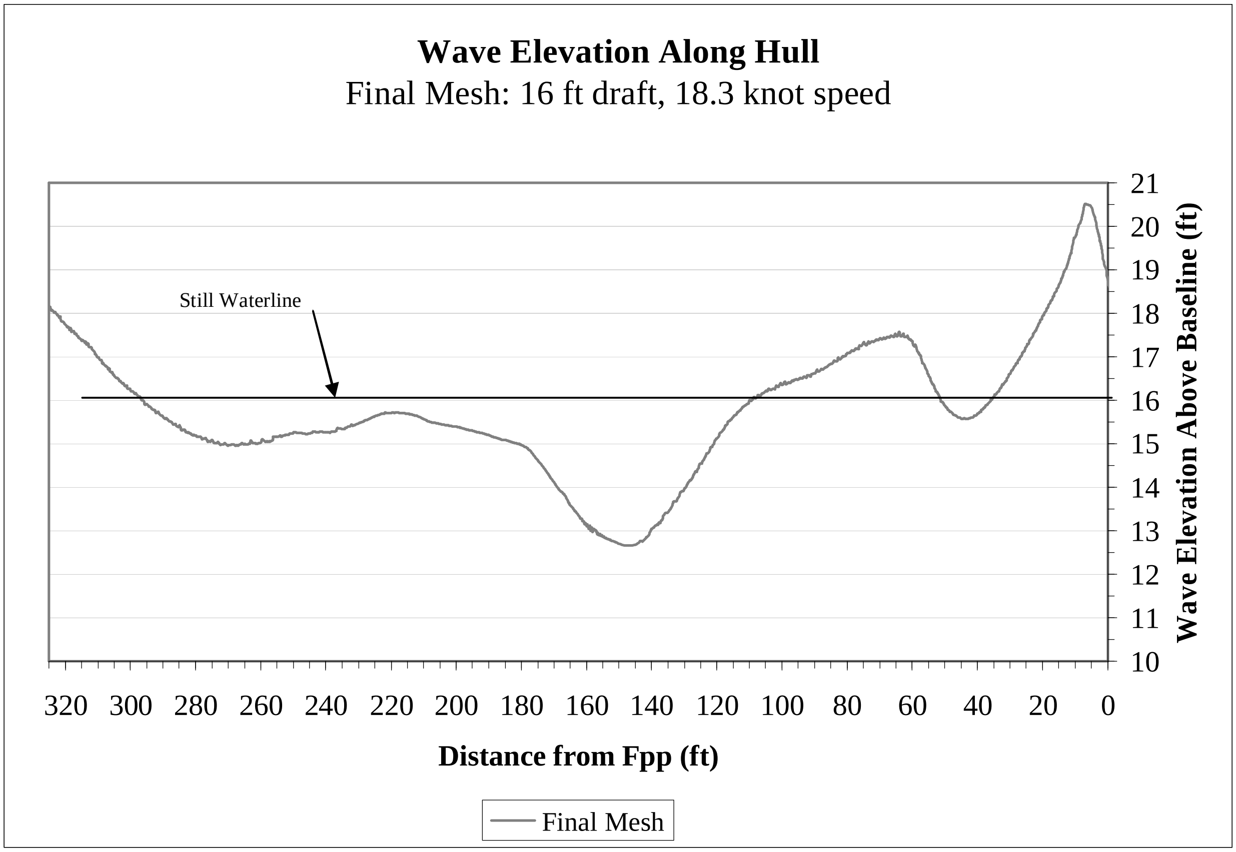

Figure B2: Free Surface Elevation along Hull

Although the vessel has a relatively small wave train, there is a fairly deep trough at about 150 ft aft of the forward perpendicular (Fpp). There is also a sharp shoulder wave being generated at about 70 ft aft of the Fpp. The bow bulb appears to be effective in reducing the amplitude and overall volume of the bow wave system.

Free Surface Elevation Contour Plots

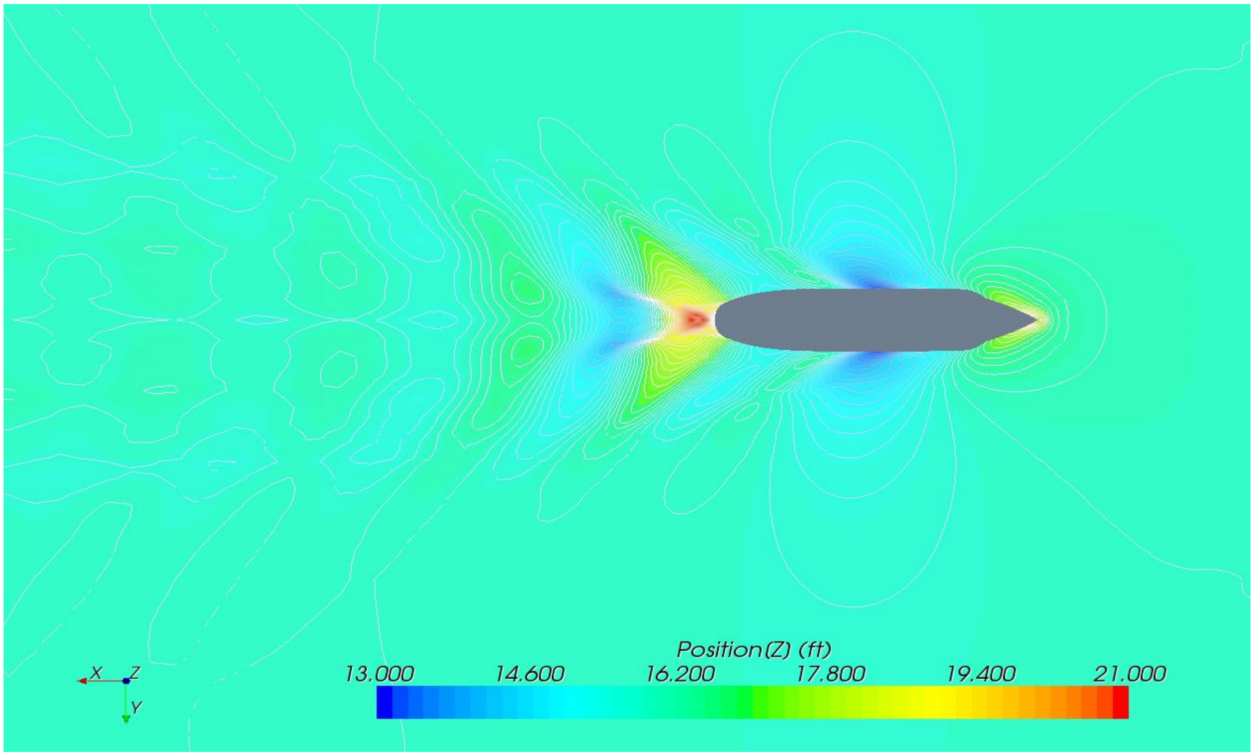

Figure B3: Far Field Wave Train, Top View

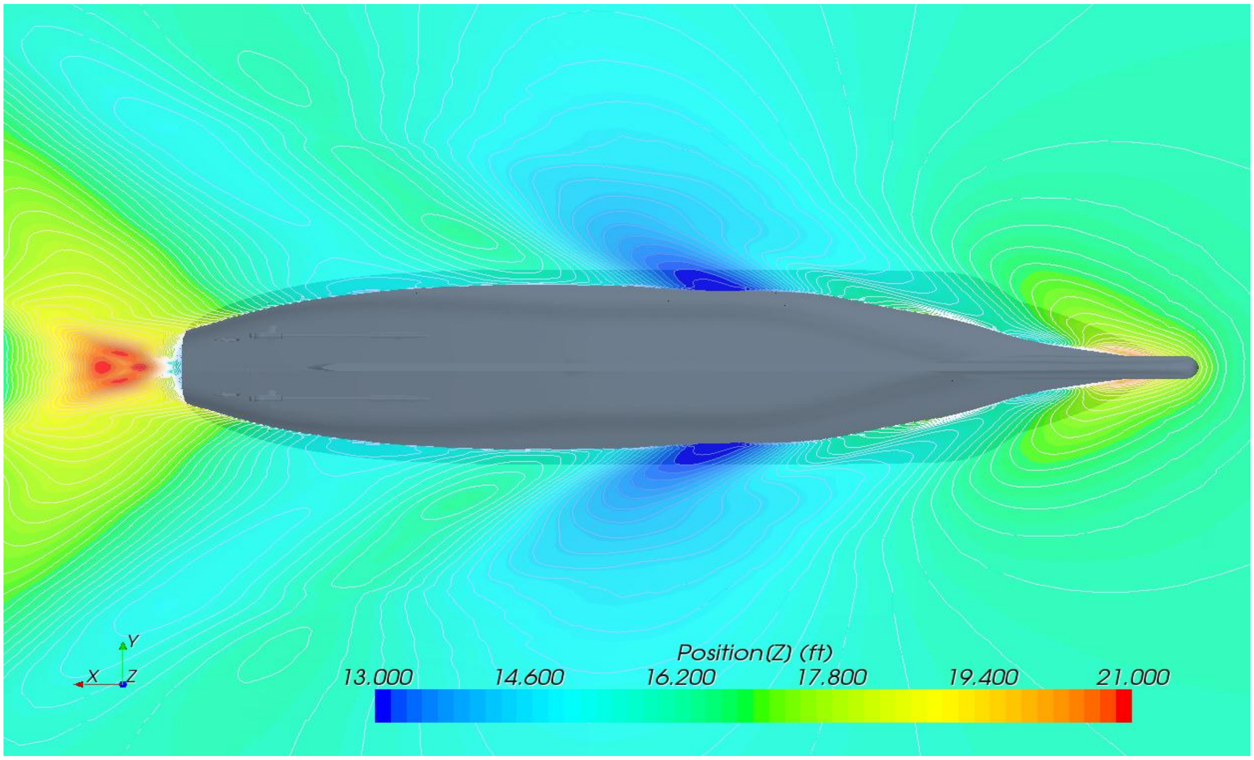

Figure B4: Near Field Wave Train, Bottom View

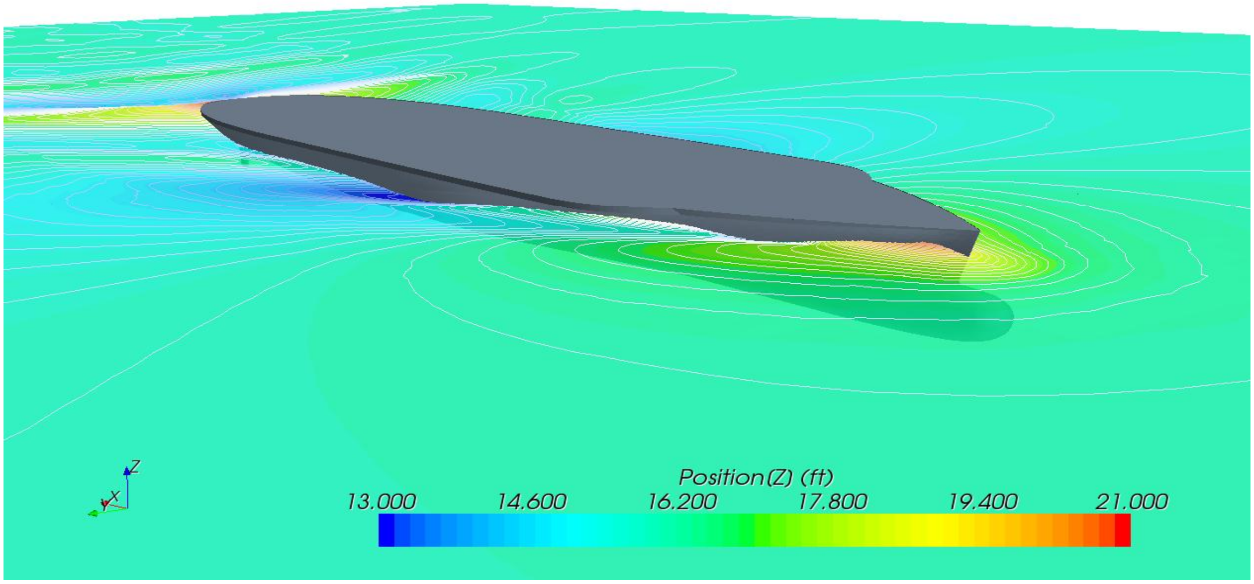

Figure B5: Free Surface, Bow Quartering View

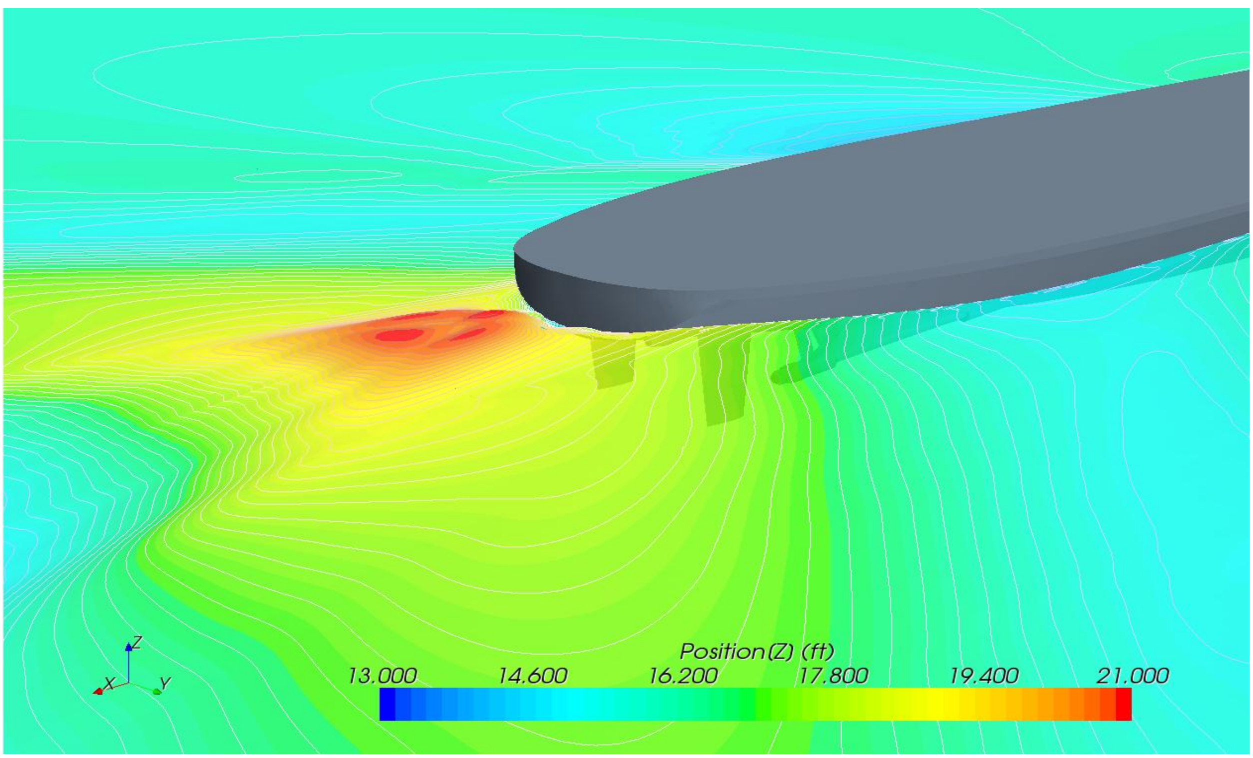

Figure B6: Free Surface, Stern Quartering View

Hull Streaklines

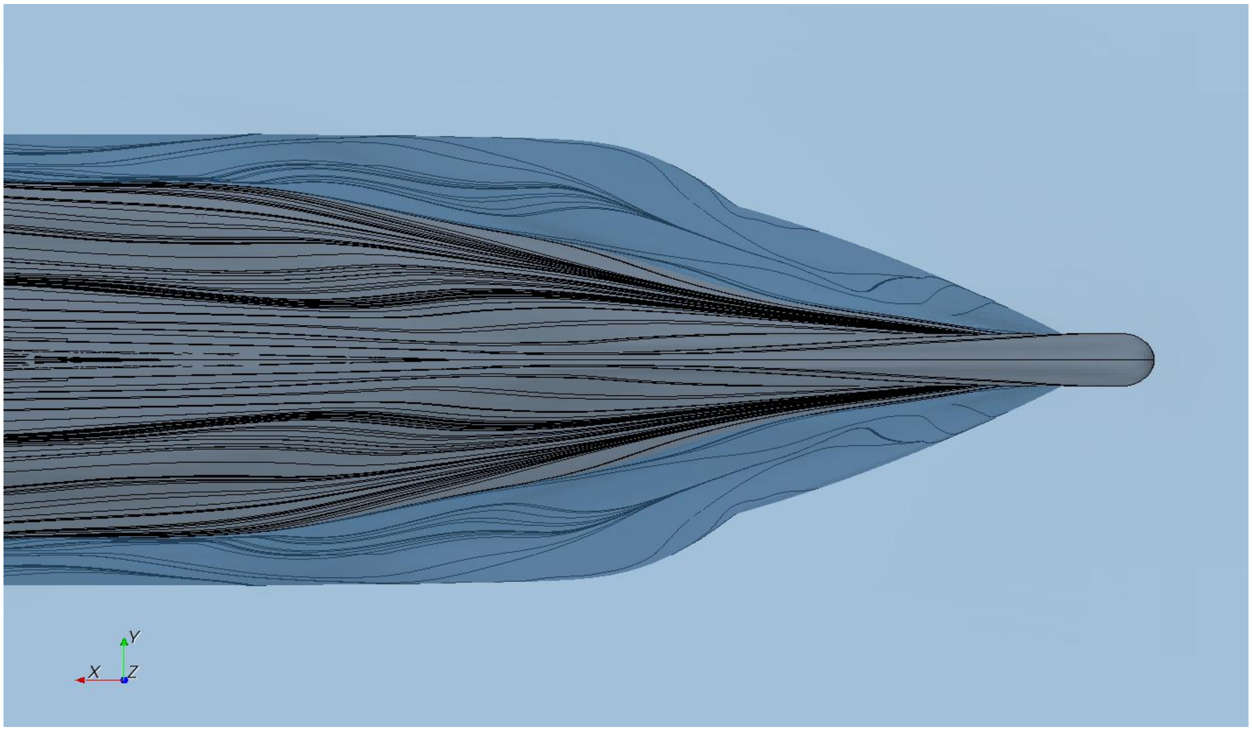

Figure B7: Streaklines, Bow Bottom View

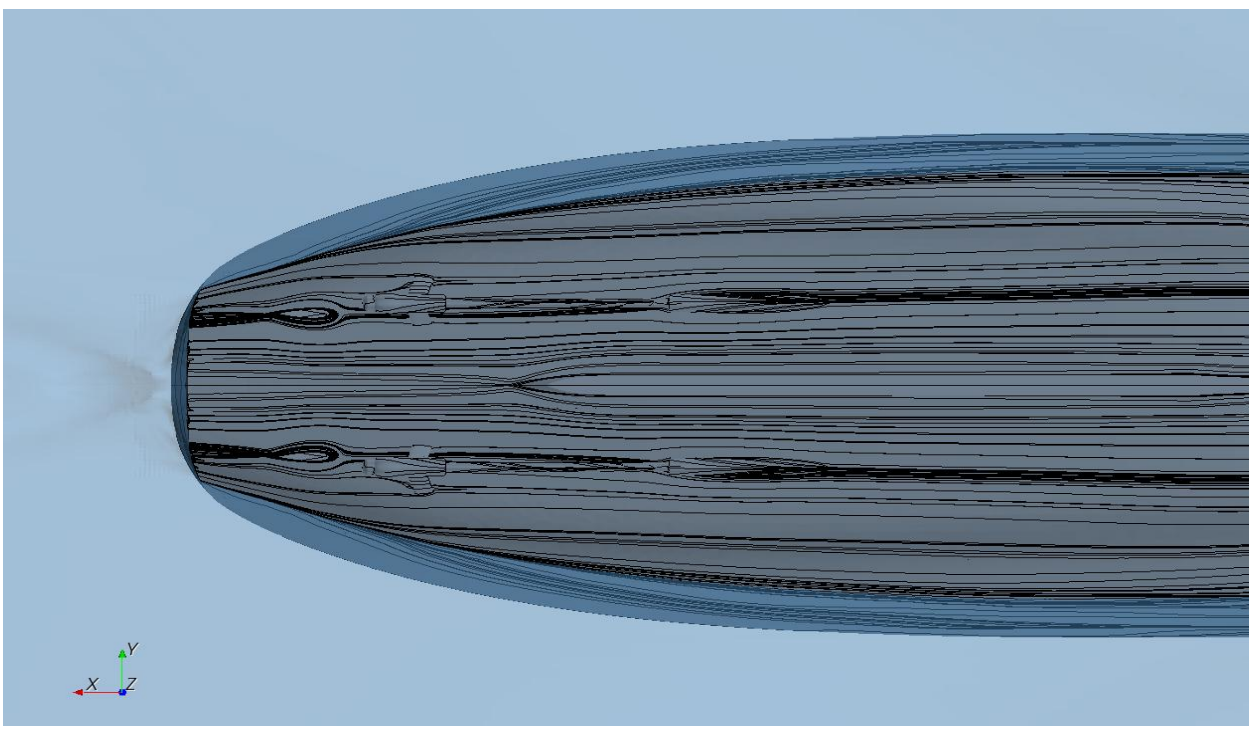

Figure B8: Streaklines, Stern Bottom View

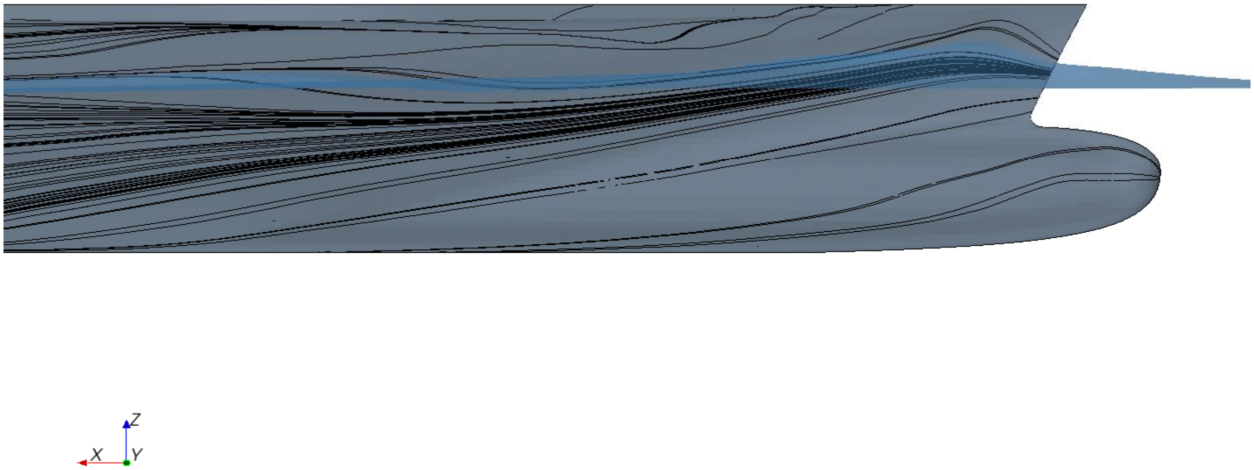

Figure B9: Streaklines, Bow Profile View

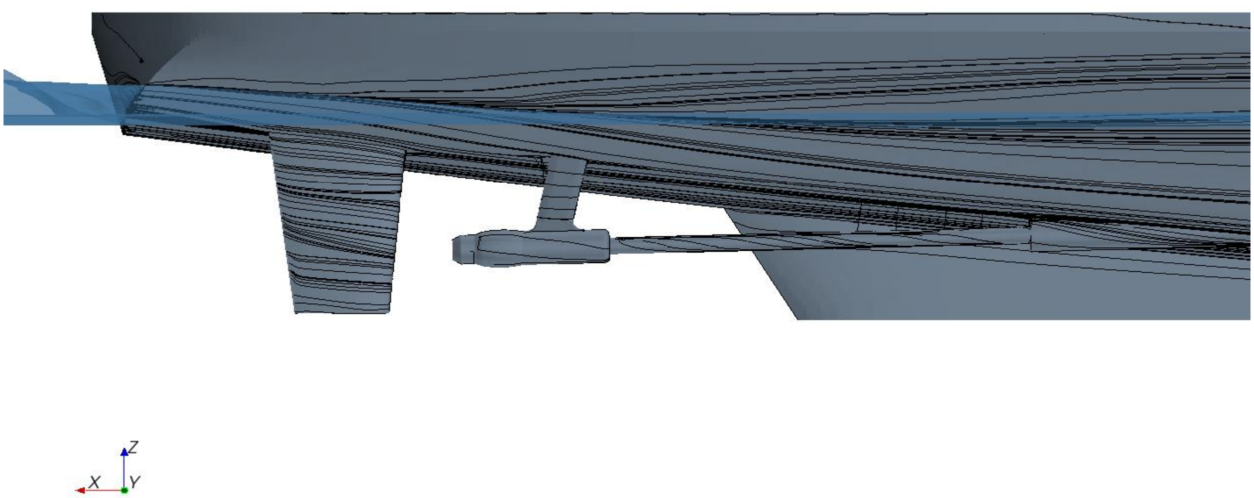

Figure B10: Streaklines, Stern Profile View

Streamlines

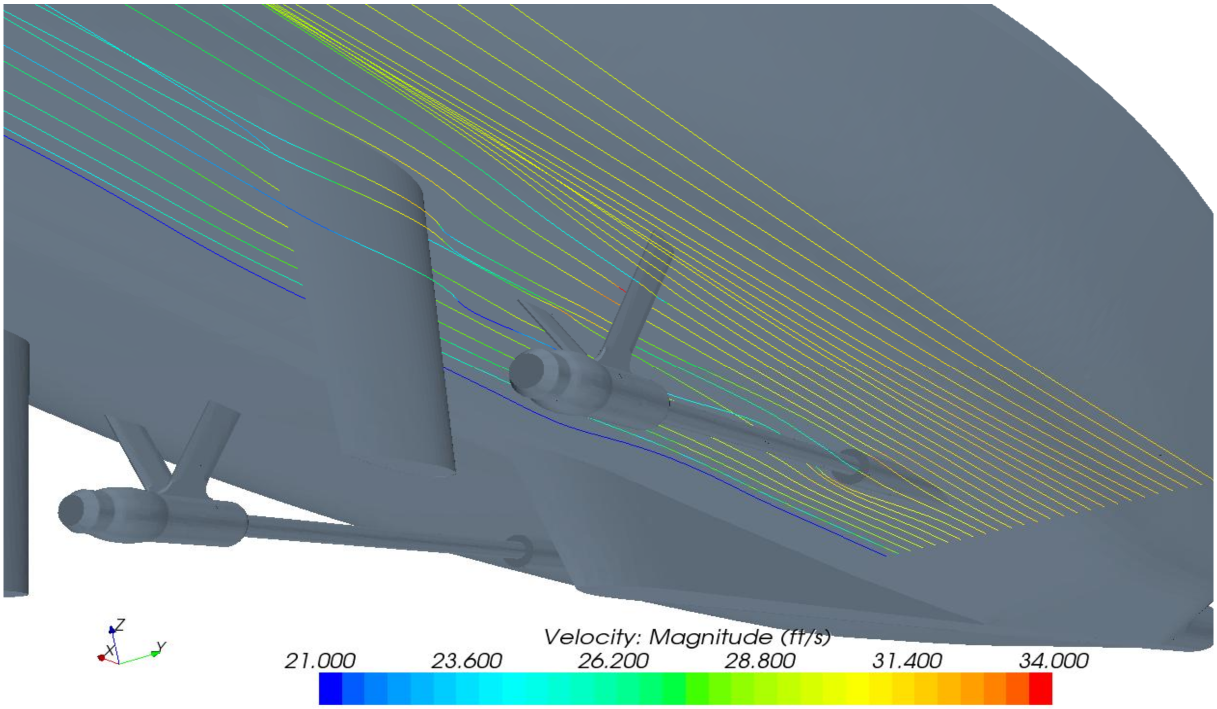

Figure B11: Appendage Streamlines, Isometric View

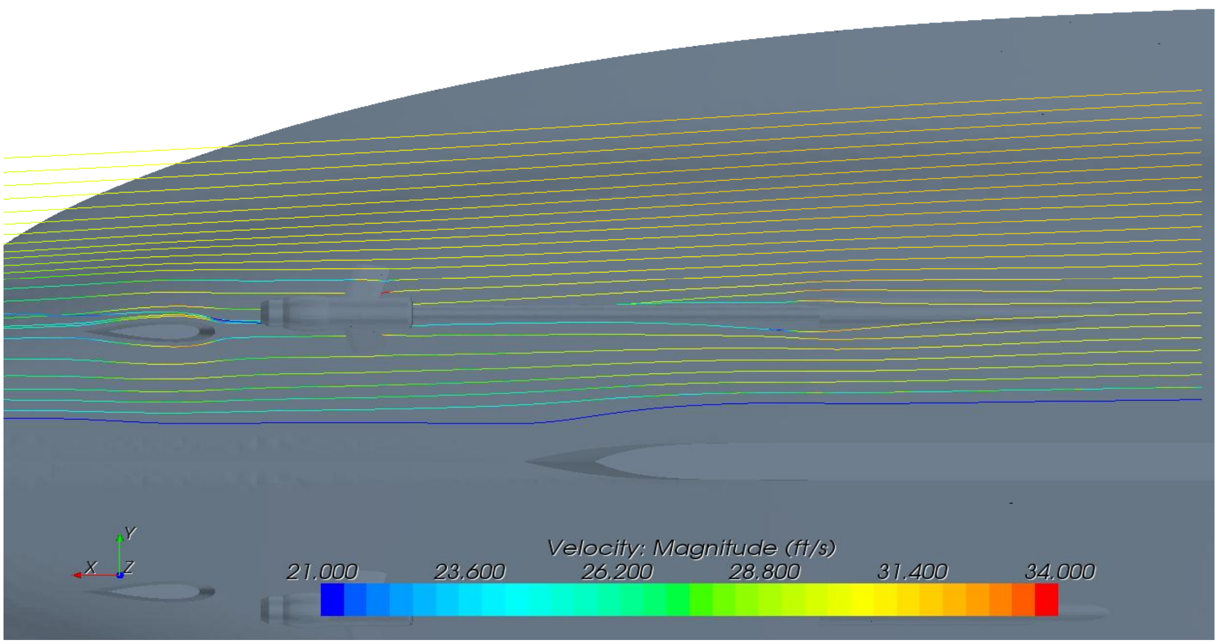

Figure B12: Appendage Streamlines, Bottom View

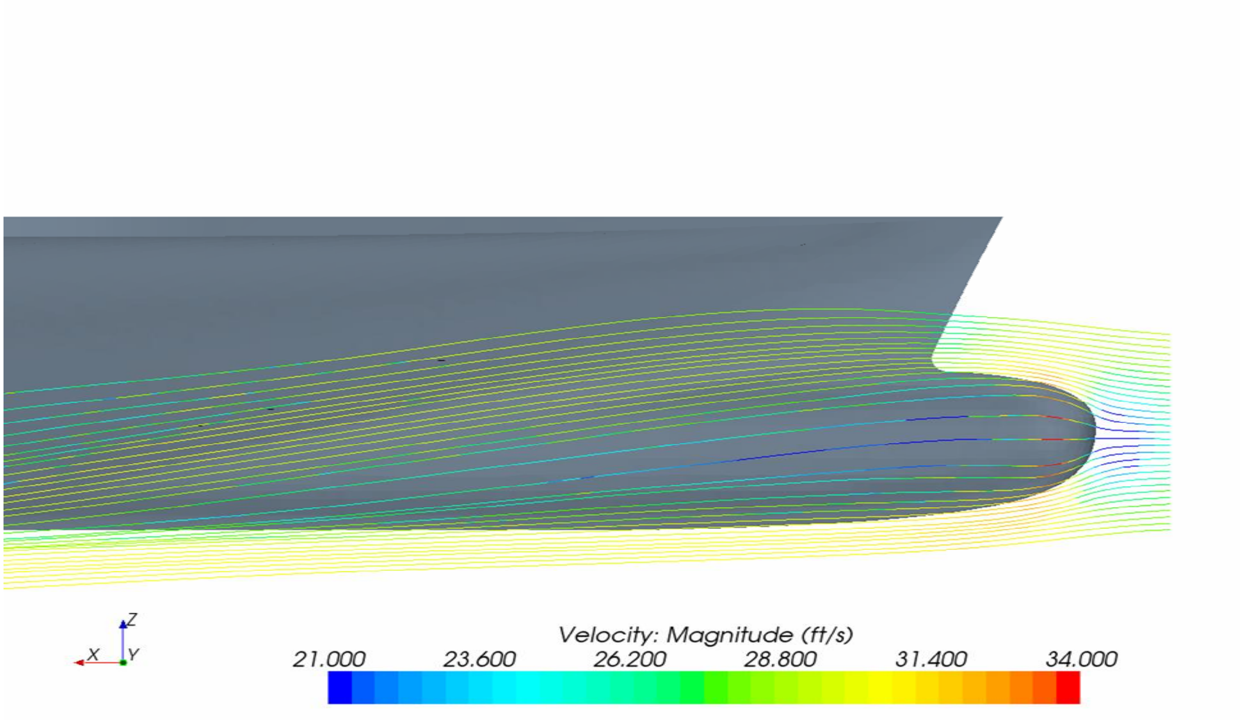

Figure B13: Bow Streamlines, Profile View

Figures B2 through B5 show contours of free surface elevation. The effects of the bulb are seen in the minimal bow wave train generated by the vessel. Figure B4 shows a rather strong quartering wave being generated at about 0.3L. Inspection of the waterlines in this area indicates that a possible improvement in the fairness of the "shoulder" of the hull may reduce the amplitude of this quartering wave. The location of this shoulder may also be amplifying the normally occurring wave trough at about midships. Improvements in the hull fairness would ideally result in a smaller amplitude wave train, which will reduce resistance.

Figures B6 through B9 show streaklines of flow, which are streamlines that have been constrained to follow the hull surface. The streakline plots are analogous to oil streak visualizations on a model test. Figures B10 through B12 show streamlines of flow in the vicinity of the hull. Streamlines in Figures B10 and B11 are released from a horizontal line with endpoint coordinates of 240, 0, 4 and 240, 30, 4 ft. Streamlines in Figure B12 are released from a vertical line with endpoint coordinates of -15, 1, 0 and -15, 1, 15 ft.

The streakline and streamline plots above show the local flow around the hull. As seen in Figures B7 and B11, the rudder and propeller shaft struts are fairly well aligned with the flow direction. Figure B12 shows the smooth streamlines of flow around the bulb and fore body of the vessel. The smoothness reflects that a fair bulb/hull intersection has been designed.

All the figures described above show the fixed model at 16.0 ft draft and 18.3 knots.

Appendix C

Computational Fluid Dynamics Procedure

Computational Fluid Dynamics Procedure Approach

The categories below describe in detail the computational fluid dynamics (CFD) procedure followed in this analysis. Once the problem scope is defined, the steps followed for a CFD analysis are: determine the appropriate level of geometrical detail and import geometry to the CFD analysis software, create a baseline solution mesh, select the appropriate physics settings, complete the systematic discretization error analysis, generate the final solution mesh, and post process the results of the final simulation.

Geometry Preparation

Vessel geometry is prepared for import into the CFD analysis software using Rhinoceros, a geometry modeling software tool. The CFD model is typically based on an existing computer model of the vessel, with modifications specific to CFD being performed. Modifications may include conversion to half-hull, removal of superstructure, removal of extraneous geometry details, addition or removal of underwater appendages, and creation of the domain extents.

A closed, high quality, three dimensional surface geometry of the vessel is required for ease of import. The vessel geometry is typically modeled from the main deck to baseline, with the superstructure not modeled for resistance studies. Superstructure geometry may need to be included for stack gas analysis or wind resistance and moment studies relating to dynamic positioning predictions. The engineer must exercise best judgment to determine what level of modeling is appropriate to include for vessel appendages and superstructure.

Solution Mesh Generation

CFD models using fully viscous three dimensional formulations are typically of the Finite Volume formulation, which requires the simulation domain to be discretized into a finite number of three dimensional volumes. Although terminology is somewhat interchangeable, the three dimensional finite "cells" make up the solution "mesh" or "grid." The governing equations are then solved for the centroids of each individual cell in the solution domain.

The solution mesh may be created using either a structured or unstructured approach. The structured approach requires a 1:1 mapping of grid points in the domain. For example, if there are 300 cells along the X axis of the domain, there must be 300 points in the X direction at any X-Y or X-Z plane section throughout the domain. This is a very restrictive condition for complex geometry, and typically results in poor quality, highly skewed cells unless great care is taken in mesh creation. Unstructured mesh types require greater computational resources and different solution formulations than the structured grids, but are much more flexible in creation as the cell counts in any direction may be varied. Unstructured mesh thus greatly simplifies mesh generation for complex geometries, and allows higher quality meshes to be created which result in greater numerical accuracy and faster computation times.

Unstructured solution mesh is used almost exclusively for modern industrial CFD analysis. The use of unstructured mesh allows the user to generate a more efficient mesh for a given number of cells, which is accomplished by clustering the greatest number (smallest) cells in regions of the flow expected or observed to contain steep gradients in velocity or turbulence. For marine vessel analysis, the areas typically requiring higher discretization include the free surface region, areas immediately around appendages and vessel geometry, and areas that are expected to contain high levels of turbulence. While the regions of high turbulence and steep gradients are not usually known a priori, experience guides the engineer to generate a baseline mesh of acceptable quality. Although the mesh generation process is inherently subjective in nature, a higher confidence level in the simulation results may be obtained by performing a formal discretization error analysis, described in the Error Analysis section.

An appropriate scale factor for the simulation is determined for each individual analysis. A scaled model may be chosen to be run in CFD for a direct comparison to physical tow tank results, or for mesh size issues. If possible, it is usually preferable to run the simulation at full scale, as this avoids conflict between Froude and Reynolds number scaling effects, which is inescapable when performing either a physical or numerical scaled model test. An appropriate solution domain size is determined for the analysis. The domain size must be large enough to avoid any significant influence of the domain boundaries on the solution, while the upper limit of domain size is chosen to avoid excessive computation time. The domain size for a typical surface vessel resistance analysis extends 1.5L forward of the vessel, 2.5L behind the vessel, 2.0D above the baseline, and 3.0D below the baseline. These domain sizing guidelines may be altered based on specific analysis requirements. The domain is sized in the transverse direction to fully capture the divergent waves generated by the vessel.

Free surface vessel simulations are further refined as follows. The mesh is stretched in the X-Y direction away from the vessel which increases cell size at greater distances from the hull surface. This effectively clusters the greatest number of cells closest to the vessel where turbulence is highest for greater accuracy. This approach also numerically damps the free surface waves at the edges of the domain which minimizes or eliminates free surface wave reflection back into the solution domain. An unstructured, trimmed hexahedron mesh is used to discretize the solution domain volume. The hexahedron mesh type is ideal for creating anisotropic refinement of the free surface in the vertical direction without being forced to needlessly refine the free surface in the horizontal plane.

Simulation Settings

Marine industry standard CFD solver settings are used for this study. The CFD program used is CD Adapco's Star-CCM+ version 4.04.011. This program has undergone rigorous verification studies related to the current analysis, and is considered capable of producing high quality results. The volume of fluid (VOF) method is used to capture the free surface interface. The second order K-Omega turbulence model with Menter's shear stress transport (SST) adaptation is used for turbulence closure of the Reynolds-Averaged Navier Stokes (RANS) equations.

The RANS equations treat turbulence as a fluctuating pressure and velocity field overlaid on a mean pressure and velocity field. The K-Omega model is an eddy viscosity model that uses the concept of turbulent viscosity to solve for the unknown turbulence quantities in terms of mean flow quantities. It should be noted that any turbulence model used in CFD is an inexact approximation of the actual flow behaviors, however for the typical industrial application the errors between the model used and actual flow behavior are acceptable provided an appropriate model is selected for the simulation. (Appendix Reference 1) The solver used is of the implicit unsteady type using first order temporal discretization for the initial flow time, after which second order temporal discretization is used. The first order approach is used for numerical stability reasons as the solution must typically iterate through an initial numerical shock early in the simulation. The first order temporal discretization is more robust and tolerates the initial numerical shock better than second order; however the second order temporal discretization is used to obtain a final resistance value due to its higher accuracy. (Appendix Reference 2)

The time step chosen for the simulation is determined using Courant number guidelines. The Courant number relates time step length, cell size, and average flow velocity. As the simulation starts iterating, there are relatively large gradients in the flow field which may result in numerical instability. To avoid instability, the time step is chosen to attain a Courant number of approximately one. As the solution converges, the Courant number may be allowed to increase by extending the time step duration, which is allowed by the implicit formulation. The implicit formulation relaxes the strict time step requirements of the explicit solver type (which requires the Courant number to be less than one for numerical stability). Although the implicit type solver is more computationally intensive for individual iterations than the explicit solver, the ability to increase the mesh size and/or the time step results in a net savings of computation time.

Near wall viscous effects are accounted for through the use of wall functions. The boundary layer is modeled using the All-Y+ wall function setting in Star-CCM+, which applies empirically derived velocity profiles within the near wall cells. Y+ is a quantity relating the cell height normal to the wall with derived flow quantities, and allows the solver to accurately account for the viscous boundary layer over the hull surface. This approach provides sufficient accuracy for high Reynolds number flows and eliminates the need to fully discretize the boundary layer, which greatly reduces the overall cell count, which in turn decreases the CPU time required to run the simulation.

Solution Convergence

Due to the existence of an evolving free surface, marine CFD analysis is run using unsteady flow formulation. The vessel resistance varies over time as a result of the flow field evolving towards a quasi-steady state. The solution is considered converged when the vessel resistance does not change appreciably over a number of time steps. Due to the nature of free surface flows, which result in the generation of gravity waves on the free surface, it is also typical to attain oscillatory convergence. Oscillatory convergence is the case where the resistance value settles into a regular oscillation about a steady value. This is due to the small, periodic fluctuations in the free surface around the vessel that occasionally persist in a quasi-steady state solution. Oscillatory convergence is usually observed for vessels that generate a breaking bow wave or highly turbulent transom wake, both of which are able to be captured by the CFD program. Ideally, the oscillation in the resistance value will reduce in amplitude as the simulation progresses to an acceptable level of fluctuation, which is determined by visual inspection of the resistance plot.

6 Degrees of Freedom

It is becoming more common in marine CFD analysis to include dynamic effects of motion into resistance analysis. The typical approach allows the simulation model to have 2 degrees of freedom (DOF) in sink and trim, although for certain cases additional degrees of freedom are required to capture the desired vessel motion.

The vessel sinks and trims due to the resulting pressure fields around the hull when the vessel is in motion. The CFD program calculates the pressure over the hull surface and applies a resultant force and moment to the hull, which is then reoriented at each time step. The mass and the moments of inertia of the vessel need to be included to allow the equations of motion to be solved. The mass is taken as the displacement of the vessel at a still water draft. Although the actual aggregate moments of inertia are usually not known early in the design phase, a parametric comparison to a similar vessel will provide a starting point for a dynamic analysis. A conservative estimate of the moments of inertia may also be obtained using a three dimensional modeling software moment of inertia output, which assumes the mass to be spread through the vessel in a constant density. The required accuracy of the moments of inertia will increase if transient vessel response is of interest, which occurs for sea keeping analyses. The goal for a sinkage and trim analysis is to reach a quasi-steady state where resistance, trim, and sinkage have converged on fairly constant values, so the moment of inertia of the vessel is not as critical.

Although the effect of sinkage and trim varies with different vessel geometry, in general for displacement hulls there is some level of sinkage along with either bow or stern trim. Sinkage will generally increase resistance slightly by combining increased wetted surface (greater frictional drag) and increased forward hull entrance angle (greater wave making and pressure drag). Dynamic trim changes may either increase or decrease vessel resistance, depending on hull configuration, speed, and magnitude of trim.

Including dynamic effects through the application of degrees of freedom to a simulation carries an additional computation burden. The equations of motion must be solved for every iteration which requires computational effort. Additionally, a shorter time step may be required for numerical stability reasons for freely moving models when compared to an equivalent fixed model. This shorter time step will require more iterations for a given physical flow time than the longer time step fixed case simulation.

Error Analysis

A formal error analysis is performed to ensure minimal impact of any modeling errors to the results. Error in numerical methods such as CFD is typically divided into three main types: model error and uncertainty, iterative error, and discretization error. Another source of error that tends to accumulate in iterative solution methods is precision error, also commonly known as round-off error, which occurs due to the computer storing values to a finite decimal place.

Modeling error and uncertainty originates in the equations used to model the fluid flow; these equations are typically linearized approximations to the governing nonlinear equations. In addition, the turbulence modeling techniques typically used are an approximation to empirically observed flow behavior.

Iterative error is the difference between a fully converged solution and an incompletely converged solution. Iterative error may be easily tracked as the solution progresses by monitoring the residuals of the governing equations. The residuals are the remainders of the governing equations that are solved during each iteration for every cell within the domain. Ideally, the residuals should reach "machine zero" which would essentially indicate a remainder of zero for each equation which corresponds to an exact solution throughout the simulation domain. The residuals should diminish as the solution progresses and moves towards convergence, with a typical reduction of three to four orders of magnitude from the initial iteration. (Appendix Reference 3)

Discretization error is mainly due to division of a solution domain volume into a finite number of cells (spatial discretization). Temporal discretization is the procedure of time marching the solution through iterative, finite time steps. As most marine CFD analysis is concerned with the quasi-steady state solution for overall vessel resistance, the time step is chosen to maximize physical solution time while maintaining numerical stability. Spatial discretization is the focus of the error analysis for this study, as it is typically the greatest contributor to overall simulation error. Discretization error is also typically the most challenging to identify, where unlike iterative error, there is no clear indicator of the impact of discretization on the solution.

To obtain a high confidence level in the solution results, the simulation must attain "mesh independence." This is the situation where changing the spatial discretization level (i.e. increasing the number of cells in the domain) results in minimal changes to the predicted vessel resistance or monitor value. A formal value for error is obtained by performing a mesh sensitivity study where the number of cells is systematically altered, and the results of each simulation compared to a baseline simulation (Appendix Reference 3). Once the error analysis has been performed, an acceptable solution error is determined and a final mesh size is established. This approach is especially useful when many simulations at various operating conditions are to be performed for a given vessel. If a large series of simulations is to be performed, it is desired to minimize the cell count to reduce calculation time without greatly increasing the discretization error.

The Grid Convergence Index (GCI) is a method for presenting discretization error. The GCI method uses an extrapolation technique to estimate the simulation result if the domain is infinitely refined. The GCI method assumes that the mesh sensitivity study has a certain order of convergence, which is a measure of how quickly the sample mesh sizes are trending towards the extrapolated result. The error of the simulation under consideration is then calculated as the difference between the extrapolated value and the current value, including an arbitrary "factor of safety."

Simulation Post Processing

The resistance of the vessel is plotted and monitored as the solution progresses. Each vessel requires a different amount of simulation time to attain a converged resistance value. This is mostly due to the differing free surface wave train generated by different vessels. Once the solution is considered converged, the resistance or monitor value of interest is exported into a spreadsheet format. The engineer will then determine an appropriate time interval to average and obtain a singular value for the desired quantity. This time interval is chosen to extend over several whole periods for oscillatory convergence, or over a representative interval for fully converged values.

One powerful aspect of CFD is the ability to generate three dimensional visualizations of many different aspects of the fluid flow. For marine analysis, it is fairly standard to present contours of free surface elevation, a plot of free surface elevation along the hull surface, and streamlines of flow around the hull and appendages. Individual analyses may be also concerned with the predicted turbulence levels in the vicinity of vessel appendages or features such as thruster tunnels and propellers. It is important to emphasize the importance of the ability to easily obtain almost any desired flow value throughout the fluid domain, as this enables the engineer to guide the vessel design development and gain valuable insight into the behavior of the flow.

Appendix References

1. Star-CCM+ User Guide Version 4.04.011, Cd-Adapco, 2009.

2. Best Practice Guidelines for Marine Applications of Computational Fluid Dynamics, MARNET-CFD group, European Union, 2003.

3. Procedure for Estimation and Reporting of Uncertainty Due to Discretization in CFD Applications, Celik, I. et al, ASME Journal of Fluids Engineering, Vol. 130, July 2008.